Synthesis and characterization of tetraammineruthenium(II) complexes bound to the bridging ligand 3,6-bis(2-pyridyl)1,2,4,5-tetrazine (bptz): comparative effects of σ and π peripheral ligands on electronic absorption and electrochemical properties

Jane E. B. Johnson, Cynthia de Groff and Ronald R. Ruminski*

Department of Chemistry, University of Colorado at Colorado Springs, Colorado Springs, CO 80933-7150 (U.S.A.)

(Received January 23, 1991; revised April 22, 1991)

Abstract

Tetraammineruthenium(II) complexes with the nitrogen aromatic heterocyclic bridging ligand 3,6-bis(2-pyridyl)1,2,4,5-tetrazine (bptz) have been prepared and characterized. The $[\{(NH_3)_4Ru\}(bptz)]^{2+}$ ion exhibits intense electronic MLCT transitions at 560(sh) and 479 nm, and for the $[\{(NH_3)_4Ru\}_2(bptz)]^{4+}$ ion MLCT transitions occur at 850(sh), 603 and 370 nm. Reversible metal oxidations for the bimetallic complex are at +1.56 and +0.72 V versus SCE and $\Delta E(2\text{–}1) = 840$ mV indicates a large degree of ruthenium–ruthenium communication occurs through the bptz bridging ligand. The energies of the MLCT transitions and electrochemical potentials are compared with those for the analogous bis-bipyridyl ruthenium bptz complexes to assess the effect of NH_3 σ versus bpy π non-bridging ligands. In these complexes, as well as others, the results show the ruthenium centers coordinated with NH_3 are comparatively π electron rich when compared with the analogous bpy complexes. ^1H and ^{13}C NMR data are reported for the bptz ligand and mono and bimetallic complexes.

Introduction

There have recently been reported a number of mono and bimetallic transition metal complexes bound through the nitrogen aromatic heterocyclic ligand 3,6-bis(2-pyridyl)1,2,4,5-tetrazine (abbreviated either as bptz or dpt) with Mn, Re, Mo, W and Ru [1–6]. Several other similar bridging ligands, such as 2,3-bis(2-pyridyl)pyrazine (dpp) [7–14], 2,3-bis(2-pyridyl)quinoxaline (dpq) [15–17], 2,2′-bipyrimidine (bpym) [1, 4, 8, 10–23], benzo[1,2-*b*:3,4-*b*′:5,6-*b*″]tripyrazine (hat) [17, 24, 25], have been used to form bidentate mono and bimetallic complexes with low spin d^6 metals. Bpym, dpp and hat bridged complexes possess highly absorbing MLCT transitions in the Vis–near-UV region of the spectrum, and metal–metal electronic interaction has been observed when the metals in polymetallic complexes are directly bound through the same ligand ring possessing good π delocalization (such as in pyrazine). Mono and bimetallic d^6 complexes bound through this type of ligand have therefore been prepared and studied as models for photochemically induced excited state energy transfer reactions, photochemistry and photophysics of polymetallic complexes, and for solvatochromic behavior.

While several research groups prepare tris-bidentate chelated metal complexes for reasons of stability and luminescence for use as bimolecular energy transfer complexes, our research group has been interested in the design and characterization of polymetallic Ru(II) complexes bound with the NH_3 peripheral ligand. Ruthenium(II)ammine complexes retain many of the necessary requirements to function in intramolecular energy transfer processes, absorb more abundant near-IR radiation, and allow for greater metal–metal electronic communication than complexes with π withdrawing non-bridging ligands.

We wish to report the synthesis and characterization of new $[\{(NH_3)_4Ru\}(bptz)](PF_6)_2$ and $[\{(NH_3)_4Ru\}_2(bptz)](PF_6)_4$ complexes, and compare electronic absorption and electrochemical results with the similar $[\{(bpy)_2Ru\}_2(bptz)](PF_6)_4$ complex and other complexes.

Experimental

Materials

Analytical reagent grade solvents and compounds were used for preparations and experiments described

*Author to whom correspondence should be addressed.

0020-1693/91/$3.50

in this work. The d_6-acetone min. 99.9 at.% D was obtained from ISOTEC inc. Elemental analyses were performed by Atlantic Microlab Inc., Atlanta, GA.

Instrumentation

Electronic absorption spectra were recorded on a Varian DMS 300 spectrophotometer with matching quartz cells. Near-IR portions of the spectrum (800–1300 nm) were recorded on a Beckman model 5240 scanning spectrophotometer. Cyclic voltammograms were recorded on a Bio Analytic Systems CV-1B cyclic voltammograph with a Princeton Applied Research model 0074 X-Y recorder. Cyclic voltammograms were recorded in CH_3CN with 0.01 M tetrabutylammonium perchlorate as the supporting electrolyte. The Pt working electrode (1.0 mm diameter) was cleaned and the solutions were thoroughly deoxygenated prior to each scan. A Ag/AgCl (3 M KCl, nominally −0.044 V versus SCE) reference electrode was used and calibrated with a $Fe(CN)_6^{4-}$ (1.0 M H_2SO_4) solution at +0.69 V versus NHE [26]. All potentials are reported versus SCE, and are uncorrected for junction potentials. The potentials reported for redox couples, $E_{1/2}$, are estimates obtained by averaging anodic and cathodic peak potentials. Emission experiments were conducted on a Hitachi model F-3210 fluorescence spectrophotometer, fitted with an extended range detector sensitive to 800 nm. ^1H and ^{13}C NMR spectra were recorded in d_6-acetone on a Varian Gemini 200 FT-NMR.

Syntheses

The bptz ligand was prepared according to the literature without difficulty [27]. *Anal.* Calc. for $C_{12}H_6N_6$ (mol mass 236.24 g): C, 61.0; H, 3.4; N, 35.6. Found: C 61.0: H, 3.4; N, 35.5%.

$[\{(NH_3)_4Ru\}(bptz)](PF_6)_2$

A 0.221 g (0.34 mmol) sample of the previously prepared $[(NH_3)_5Ru(H_2O)](TFMS)_3$ (TFMS = $CF_3SO_3^-$) complex [28], 0.416 g (1.76 mmol) of bptz, Zn/Hg amalgam and 0.100 dm^3 of anhydrous ethanol, were combined in a round bottom flask fitted with a condenser (top closed with a septum and an Ar inlet needle). The solution was heated at reflux for 1.5 h. After cooling to room temperature, the red solution was filtered to remove insoluble material, and the liquor loaded onto an alumina column that had been packed in ethanol. The column was washed with ethanol to remove unreacted ligand, followed by a NH_4PF_6/methanol solution (0.5 g/1.00×10^{-1} dm^3) that moved a red band, followed by a blue band from the column. The red was collected, and rotary evaporated to dryness. The solid, which contained excess NH_4PF_6, was collected, washed with cold H_2O, and vacuum dried. Yield $[\{(NH_3)_4Ru\}(bptz)](PF_6)_2\cdot CH_3OH$: 0.074 g (0.01 mmol) 30%, average yield is dependent upon amount of washing. *Anal.* Calc. for $C_{13}H_{24}N_{12}O_1RuP_2F_{12}$ (mol mass 727.38 g): C, 21.5; H, 3.3; N, 19.2. Found: C 21.4: H, 3.1; N, 18.9%.

$[\{(NH_3)_4Ru\}_2(bptz)](PF_6)_4$

A 0.400 g (0.615 mmol) sample of $[(NH_3)_5Ru(H_2O)](TFMS)_3$, 0.353 g (0.149 mmol) bptz, Zn/Hg amalgam and 0.100 dm^3 of anhydrous ethanol were combined in a round bottom flask fitted with a condenser (top closed with a septum and an Ar inlet needle). The solution was heated at reflux for 3 h. After cooling to room temperature, the solid was collected by filtration, washed with ethanol to remove excess ligand and monometallic complex. The compound was dissolved in water, and precipitated upon addition of a saturated aqueous $NaPF_6$ solution. The solid was collected by filtration, washed with cold water then ethanol and vacuum dried. Yield $[\{(NH_3)_4Ru\}_2(bptz)](PF_6)_4$: 0.084 g (0.073 mmol) 49%. *Anal.* Calc. for $C_{12}H_{30}N_{14}Ru_2P_4F_{24}$ (mol mass 1154.5 g): C, 12.5; H, 2.8; N, 17.0. Found: C, 12.8; H, 2.7; N, 16.7%.

Results

The aqueous $[\{(NH_3)_4Ru\}(bptz)]^{2+}$ ion exhibits intense transitions between 750–250 nm (Table 1, Fig. 1). The lowest energy aqueous transition is a shoulder at 560 nm on a more intense peak at 479 nm. A higher energy peak occurs at 295 nm. The aqueous $[\{(NH_3)_4Ru\}_2(bptz)]^{4+}$ ion exhibits intense transitions between 900–250 nm (Table 1, Fig. 1). The lowest energy transition for the aqueous bimetallic complex appears as a shoulder at 850 nm on the side of a more intense peak at 603 nm. Higher energy peaks are observed at 370 and 299 nm. The $[\{(NH_3)_4Ru\}_{1,2}(bptz)]^{2+,\,4+}$ ions were found to be non-emissive in deoxygenated room temperature CH_3CN.

Cyclic voltammograms of $[\{(NH_3)_4Ru\}_{1,2}(bptz)]^{2+,\,4+}$ were recorded in CH_3CN (Table 1). The monometallic complex exhibits one reversible redox wave associated with the Ru(II)/Ru(III) couple when scanned in a positive direction, while the bimetallic complex shows two well resolved waves for each Ru(II)/Ru(III) center (Fig. 2). The $E_{1/2}$ for $[\{(NH_3)_4Ru\}(bptz)]^{2+}$ at +1.27 V (all potentials reported versus SCE) is more positive than $E_{1/2}(1) = +0.72$ V for the bimetallic $[\{(NH_3)_4Ru\}_2(bptz)]^{4+}$ complex, while $E_{1/2}(2)$, the redox cou-

TABLE 1. Aqueous electronic absorption and electrochemical data for some ruthenium(II) complexes

Complex ion	λ_{max} (nm)	$\epsilon \times 10^{-3}$ (M^{-1} cm^{-1})	Assignment	$E_{1/2}(2)$; $E_{1/2}(1)$; E_{red}	Reference
$[\{(NH_3)_4Ru\}(bptz)]^{2+}$	560(sh)	4.6	MLCT	+1.27; −0.76	this work
	479	7.9	MLCT		
	295	28	$\pi \rightarrow \pi^*$		
$[\{(NH_3)_4Ru\}_2(bptz)]^{4+}$	850(sh)	(6)	MLCT	+1.56; +0.72; −0.70; −1.49	this work
	603	19	MLCT		
	370	7.4	MLCT		
	299	36	$\pi \rightarrow \pi^*$		
$[\{(bpy)_2Ru\}_2(bptz)]^{4+}$	688				1
	683	12	MLCT	+2.02; +1.52; −0.03; −1.25(irr)	2, 5
	577	5	MLCT		
	463	3.5	MLCT		
	411	7.5	MLCT		
	291	31	$\pi \rightarrow \pi^*$		
$[\{(NH_3)_3Ru\}(tpd)]^{2+}$	550(sh)	3.1	MLCT	+0.97	29
	492	6.4	MLCT		
	380	4.5	MLCT		
	330	34	$\pi \rightarrow \pi^*$		
$[\{(NH_3)_3Ru\}_2(tpd)]^{4+}$	582	19	MLCT	+1.31; +0.81	29
	430	6.7	MLCT		
	380(sh)		MLCT		
	350	35	$\pi \rightarrow \pi^*$		
$[\{(NH_3)_4Ru\}(dpp)]^{2+}$	545	4.5	MLCT		9
	454	4.8	MLCT		
	368	5.0	MLCT		
	307	17	$\pi \rightarrow \pi^*$		
$[\{(NH_3)_4Ru\}_2(dpp)]^{4+}$	558	19	MLCT		9
	368	9.8	MLCT		
	318	25	$\pi \rightarrow \pi^*$		
$[\{(NH_3)_4Ru\}(bpym)]^{2+}$	567	2.0	MLCT		18
	402	8.4	MLCT		
$[\{(NH_3)_4Ru\}_2(bpym)]^{4+}$	697	4.0	MLCT		18
	424	18	MLCT		

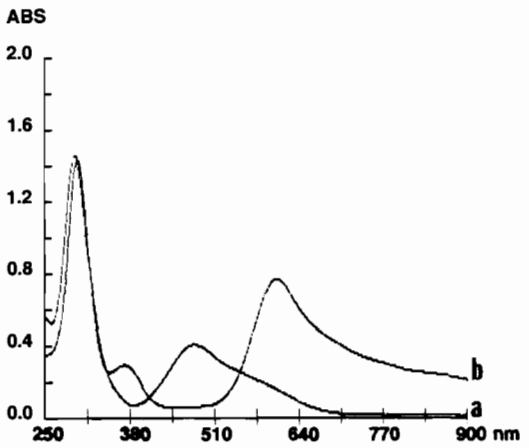

Fig. 1. Aqueous electronic absorption spectra for $[\{(NH_3)_4Ru\}(bptz)]^{2+}$ (a) and $[\{(NH_3)_4Ru\}_2(bptz)]^{4+}$ (b).

ple of the second Ru in the bimetallic complex, occurs at +1.56 V. The most positive bptz reduction potentials are reversible and occur at −0.70 and −0.76 V, respectively, for the bimetallic and monometallic complexes. The bimetallic complex also has a second reversible reduction at −1.49 V, followed by an irreversible wave at −1.55 V.

Titration of $[\{(NH_3)_4Ru\}_2(bptz)]^{4+}$ (c. 5×10^{-5} M) with additions of up to one equivalent Ce(IV) produced a decrease in absorbance of the long wavelength shoulder, 603 and 370 nm peaks, with the appearance of a 495 nm absorption (Fig. 3(a)). Throughout Ce(IV) additions up to one equivalent to form the Ru(II):Ru(III) species no absorptions were observed in the 700–1300 nm region, while isosbestic points were established at 545 and 365 nm. Addition of up to the second equivalent of Ce(IV) to produce the Ru(III):Ru(III) species re-

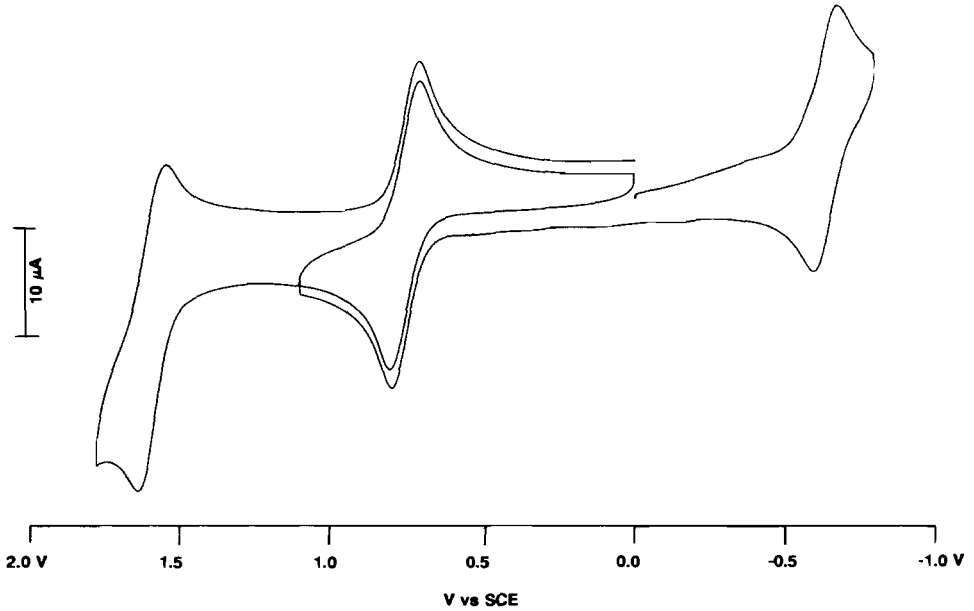

Fig. 2. Cyclic voltammograph of $[\{(NH_3)_4Ru\}_2(bptz)]^{4+}$ in CH_3CN 0.01 M TBAP at Pt working electrode vs. SCE.

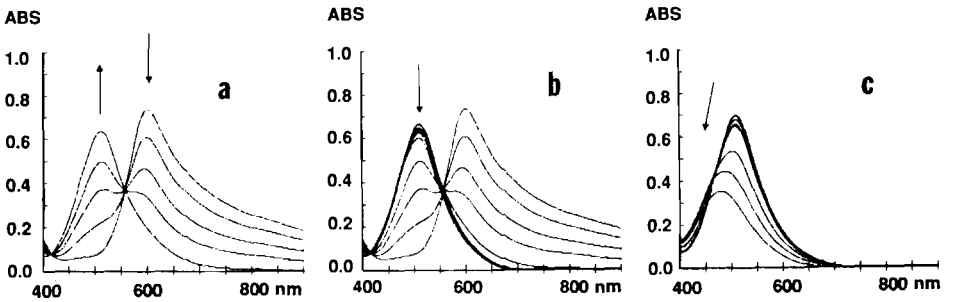

Fig. 3. Plots of Ce(IV) additions to a solution of $[\{(NH_3)_44Ru\}_2(bptz)]^{4+}$. (a) The initial spectrum and 25%, 50%, 75% and 100% of one equivalence of Ce(IV) added. (b) Followed by 25%, 50%, 75% and 100% of a second equivalence of Ce(IV) added. (c) Excess Ce(IV) added after the first and second equivalence.

sulted a slight decrease in the 495 nm peak, and formation of a different set of isosbestic points (Fig. 3(b)). Excess Ce(IV) additions past two equivalents resulted in the gradual decrease of absorption intensity near 495 nm, and absorption shift to higher energy (Fig. 3(c)). Following oxidation of the bimetallic complex to either Ru(II):Ru(III) or Ru(III):Ru(III), additions of Sn(II) (followed by filtration) or Zn/Hg regenerated the original absorption spectrum of the Ru(II):Ru(II) bimetallic complex. Additions of Sn(II) to solutions in which more than two equivalents of Ce(IV) had been added failed to regenerate the original bimetallic Ru(II):Ru(II) spectrum.

The ^1H and ^{13}C NMR spectra of bptz (Fig. 4), $[\{(NH_3)_4Ru\}(bptz)]^{2+}$ and $[\{(NH_3)_4Ru\}_2(bptz)]^{4+}$ were recorded in d_6-acetone for maximum solubility, and results are reported in Table 2. The uncoordinated bptz ligand gives four sets (two doublets, one triplet and a doublet of doublets) of ^1H and four ^{13}C NMR signals. The symmetric bimetallic complex also gives the same pattern of four sets of ^1H and four ^{13}C resonances. The ^1H NMR spectrum for unsymmetric monometallic complex gives four distinct sets of doublets, two distinct sets of triplets and an overlapping set of triplets. The ^{13}C NMR spectrum of the monometallic complex has eight resonances due to the non-equivalent quaternary carbons.

Discussion

The Vis–UV spectrum for $[\{(NH_3)_4Ru\}(bptz)]^{2+}$ is similar to spectra previously reported for $[\{(NH_3)_{3,4}Ru\}(LL)]^{2+}$ (where LL = dpp, bpym and the tridentate ligand tpd) [9, 18, 29, 30]. Due to the intensity and position of the lowest energy absorptions, they are assigned as Ru $d\pi \rightarrow$ bptz $p\pi^*$

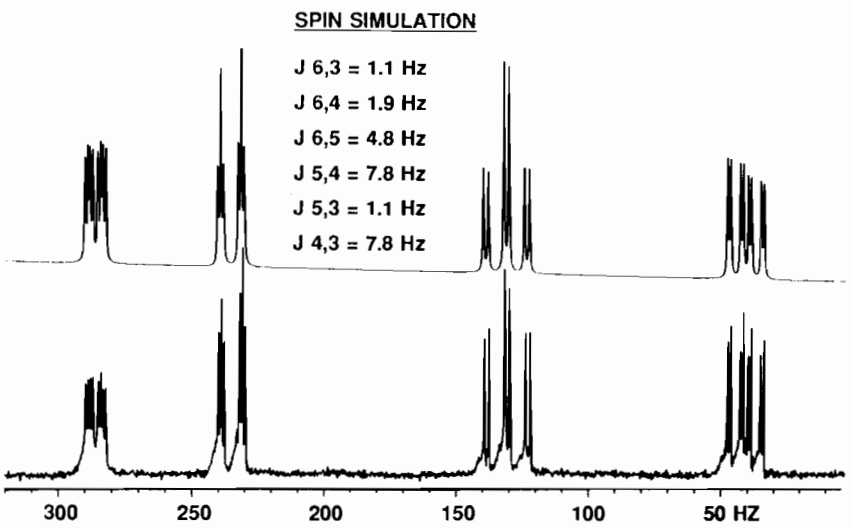

Fig. 4. Proton NMR of the uncoordinated bptz ligand (bottom) and simulated NMR (top) with coupling constants.

TABLE 2. ^{1}H and ^{13}C NMR signals of bptz, $[\{(NH_3)_4Ru\}(bptz)]^{2+}$ and $[\{(NH_3)_4Ru\}_2(bptz)]^{4+}$ complexes

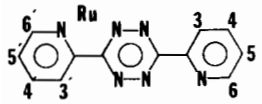

Complex ion	$\delta(^{13}C)$ (ppm)[a]				$\delta(^{1}H)$ (ppm)				$J_{6,5}$	$J_{5,4}$	$J_{4,3}$	$J_{6,4}$	$J_{5,3}$	$J_{6,3}$
	C_6 $C_{6'}$	C_5 $C_{5'}$	C_4 $C_{4'}$	C_3 $C_{3'}$	H_6 $H_{6'}$	H_5 $H_{5'}$	H_4 $H_{4'}$	H_3 $H_{3'}$						
bptz	151.3	124.8	138.0	126.9	8.93	7.69	8.15	8.68	4.8	7.8	7.8	1.9	1.1	1.1
$[\{(NH_3)_4Ru\}_2(bptz)]^{4+}$	154.1	126.1	137.0	128.6	9.06	7.78	8.07	8.84	5.4	7.7	7.7	1.8	1.1	[b]
$[\{(NH_3)_4Ru\}(bptz)]^{2+}$	150.9	124.9	138.4	127.2	8.88	7.68	8.11	8.60	4.5	7.8	7.6	2.0	1.2	[b]
	154.0	125.3	137.9	128.6	8.97	7.84	8.15	8.66	4.9	7.4	7.8	2.0	1.2	1.2

[a] ^{13}C and ^{1}H chemical shifts in d_6-acetone, $\delta = 206.04$ and 2.04 ppm vs. TMS. [b] Not clear enough to measure.

MLCT transitions. The 295 nm ($\epsilon = 2.8 \times 10^4$ M^{-1} cm^{-1}) peak is assigned as a intraligand $p\pi \rightarrow p\pi^*$ transition based on the large molar absorptivity, and similarity with the $[\{(bpy)_2Ru\}_2(bptz)]^{4+}$ ion [1, 2, 5].

The similarity of $[\{(NH_3)_4Ru\}_2(bptz)]^{4+}$ with the previously reported $[\{(bpy)_2Ru\}_2(bptz)]^{4+}$ complex allows for evaluation of the comparative electronic absorption and electrochemical effects of the σ only NH_3 versus π backbonding bpy non-bridging ligands.

The 850 nm shoulder, and gradual rise to the 603 nm peak for $[\{(NH_3)_4Ru\}_2(bptz)]^{4+}$ may contain several MLCT transitions. Near-IR and low energy visible absorptions have also been reported for bptz bridged bimetallic Mo(0), W(0), Re(I) and Mn(I) carbonyl complexes [2, 3, 6], as well as for the $[\{(bpy)_2Ru\}_2(bptz)]^{4+}$ ion [5]. Previous assignment of low energy absorptions as MLCT transitions for carbonyl complexes was based on solvatochromic behavior, and for $[\{(bpy)_2Ru\}_2(bptz)]^{4+}$, on ESR data. The absorption peak at 688 nm for $[\{(bpy)_2Ru\}_2(bptz)]^{4+}$ was assigned as a $d\pi \rightarrow$ bptz $p\pi^*$ MLCT transition. The higher energy absorptions were assigned to Ru $d\pi$ transitions as higher unoccupied MOs, and Ru $d\pi \rightarrow$ bpy $p\pi^*$ MLCT transitions to a 404 nm absorption.

A comparison of the lowest MLCT transition energies of $[\{(NH_3)_4Ru\}_2(bptz)]^{4+}$ versus $[\{(bpy)_2Ru\}_2(bptz)]^{4+}$ shows the MLCT shoulder at 850 nm for the ammine complex lower in energy than the corresponding shoulder at 800 nm for the bis-bpy complex. This is in agreement with previous comparisons for ruthenium ammine versus bpy complexes utilizing bpym [18] and dpp [9] as bridging ligands, and ammine versus tpy ruthenium(II) complexes with tpd [29, 30] as the bridging ligand. Since the σ only

NH_3 ligand has no interaction with the filled Ru $d\pi$ orbitals, they are effectively non-bonding and comparatively de-stabilized with respect to the Ru $d\pi$ orbitals in complexes bound to the π withdrawing bpy ligands. As a result, a lower energy Ru $d\pi \rightarrow$ bptz $p\pi^*$ MLCT transition is observed for the ammine complexes. Of particular interest is the 603 nm peak for $[\{(NH_3)_4Ru\}_2(bptz)]^{4+}$ that is *higher* in energy than the similar 688 nm peak for $[\{(bpy)_2Ru\}_2(bptz)]^{4+}$. Our interpretation of the results is that for the $[\{(NH_3)_4Ru\}_2(bptz)]^{4+}$ complex, the Ru $d\pi \rightarrow$ bptz $p\pi^*$ MLCT transition at 603 nm is essentially localized to the tetrazine ring with minimal or no π mixing of the bptz tetrazine–pyridine rings. This is attributed to the fact that the coordinated pyridine rings do not compete for π electron density with the peripheral NH_3 ligands. In contrast for the $[\{(bpy)_2Ru\}_2(bptz)]^{4+}$ complex, the coordinated pyridyl rings of the bptz bridging ligand compete for electron density through the Ru $d\pi$ orbitals with the bpy peripheral ligands, and the comparatively reduced amount of electron density allows for more effectively mixing of the bptz pyridine and tetrazine rings. It is the enhanced pyridine–tetrazine interaction that lowers the second highest bptz unoccupied molecular orbital of the $[\{(bpy)_2Ru\}_2(bptz)]^{4+}$ complex, resulting in a comparatively lower MLCT energy.

Electrochemical results support the interpretation that the tetrazine ring of bptz does not undergo significant interaction with the pyrazine rings in the $[\{(NH_3)_4Ru\}_2(bptz)]^{4+}$ complex. Previous studies have correlated the separation of the first and second reductions of the bridging ligand in bimetallic complexes to the effective number of bonds in the bridging ligand system [31]. Bridging ligand systems with high numbers of bonds (delocalized poly-ringed systems) are able to minimize columbic repulsions while bridging ligand systems with a small number of bonds (localized or non-coupled ring systems) are unable to separate charge to reduce columbic repulsions. The 790 mV separation of the first two bptz reductions for $[\{(NH_3)_4Ru\}_2(bptz)]^{4+}$ corresponds to a system with less than 10 bonds, that is, localized to the central tetrazine ring with little interaction to the pyridine rings.

The tentative assignment of absorptions for $[\{(NH_3)_4Ru\}_2(bptz)]^{4+}$ is that the 850 nm shoulder is assigned as a Ru $d\pi \rightarrow$ bptz $p\pi^*$ MLCT transition to the lowest unoccupied bptz molecular orbital and the 603 nm peak a Ru $d\pi \rightarrow$ bptz $p\pi^*$ MLCT transition to a higher unoccupied molecular orbital also localized to the tetrazine ring. The 370 nm transition is assigned as a higher energy Ru $d\pi \rightarrow$ bptz $p\pi^*$ MLCT transition, while the 299 nm absorption is similar in energy and intensity to that reported for $[\{(bpy)_2Ru\}_2(bptz)]^{4+}$ and is assigned as a bptz π–π^* intraligand transition.

The low energy shift of the MLCT transition for bimetallic versus monometallic complexes has previously been observed for low spin d^6 systems, and has been interpreted as being duc to a combination of the lowering of the bridging ligand π^* LUMO and formation of a higher energy Ru $d\pi$-bridging ligand $p\pi^*$–Ru $d\pi$ non-bonding molecular orbital [7, 9, 18, 32, 33]. The net result observed is a lower energy $d\pi$(non-bonding) $\rightarrow p\pi^*$ transition in bimetallic complexes. Electrochemical measurements verify the bptz $p\pi^*$ LUMO for $[\{(NH_3)_4Ru\}_2(bptz)]^{4+}$ is 0.06 V more easily reduced (stabilized), and the $d\pi$ HOMO is 0.55 V more easily oxidized (destabilized) than in the $[\{(NH_3)_4Ru\}(bptz)]^{2+}$ complex. The less positive potential of $E_{1/2}(1)$ for $[\{(NH_3)_4Ru\}_2(bptz)]^{4+}$ versus $E_{1/2}$ for $[\{(NH_3)_4Ru\}(bptz)]^{2+}$ by 0.55 V can be attributed to predominate $(NH_3)_4Ru$ $d\pi$ back-donation to the bptz ligand, resulting in formation of a Ru $d\pi$–bptz $p\pi^*$–Ru $d\pi$ non-bonding molecular orbital that is more easily oxidized.

The ruthenium redox potentials $E_{1/2}(1)$ and $E_{1/2}(2)$ for the $[\{(NH_3)_4Ru\}_2(bptz)]^{4+}$ couples are less positive than the analogous $[\{(bpy)_2Ru\}_2(bptz)]^{4+}$ couples. This follows from the concept that the NH_3 ligands do not withdraw Ru $d\pi$ electron density as do the bpy ligands, resulting in less positive metal oxidations for the ammine complex. The value of $\Delta E_{1/2}(2\text{–}1) = 840$ mV for $[\{(NH_3)_4Ru\}_2(bptz)]^{4+}$ is larger than the $\Delta E_{1/2}(2\text{–}1) = 500$ mV value for $[\{(bpy)_2Ru\}_2(bptz)]^{4+}$, and the magnitude of the $\Delta E_{1/2}$ indicates substantial metal–metal interaction occurs for both complexes. The larger $\Delta E_{1/2}$ value for the ammine complex indicates enhanced Ru–Ru interaction may result from radial extension of the $d\pi$ orbitals in the presence of σ bonding peripheral ligands such as NH_3, versus π competitive bpy ligands. The smaller $\Delta E_{1/2}(2\text{–}1) = 500$ mV value for the $[\{(bpy)_2Ru\}_2(bptz)]^{4+}$ again indicates that π competitive peripheral ligands compete for electron density, resulting in less electronic communication between the metal centers. As previously demonstrated, it is the electron density at the coordination centers in the LUMO of the bridging π ligand that determine the $\Delta E_{1/2}(2\text{–}1)$ value [4]. Our interpretation of the data is consistent with that concept since the comparatively rich Ru $d\pi$ orbitals with NH_3 as the peripheral ligands allow for greater electron density at the tetrazine coordinating atoms, resulting in the large metal–metal interaction for the ammine complex.

The $\Delta E_{1/2}(2-1)$ values of the bimetallic complex allow for the calculation of K_{com} according to the formula $\exp^{(\Delta E_{1/2}(2-1)/25.69)}$, where $\Delta E_{1/2}$ is in millivolts and $T = 25$ °C, and the comproportionation equilibrium is described by [34–36]

$$\{(NH_3)_4Ru\}_2(bptz)^{4+} + \{(NH_3)_4Ru\}_2(bptz)^{6+} \longrightarrow 2\{(NH_3)_4Ru\}_2(bptz)^{5+}$$

The $K_{com} = 1.6 \times 10^{14}$ value is larger than the calculated value for the analogous tetraammineruthenium bpym [18] and dpp [9] bridged complexes. Despite the high comproportionation constant, titration of the $[\{(NH_3)_4Ru\}_2(bptz)]^{4+}$ [2+, 2+] species with Ce(IV) produced a decrease of the characteristic absorptions at 850, 603 and 370 nm without appearance of an intervalence band in the 700–1300 nm region. The ability to detect intervalence absorptions was limited by the large extinction coefficients of MLCT transitions of the reactant and by the solvent window. Thus experimental conditions limit the ability to detect an intervalence band to transitions with $\epsilon > 10^3$, and a water solvent limited wavelength window to $\lambda < 1300$ nm. Throughout Ce(IV) addition up to one equivalent, isosbestic points at 545 and 365 nm observed during the 495 nm absorption increase, indicated formation of a single product, that was most likely the $[\{(NH_3)_4Ru\}_2(bptz)]^{5+}$ species. Throughout addition of the second equivalent of Ce(IV), the second set of isosbestic points established as the absorption maximum at 495 nm decreased in intensity, is interpreted as the $[\{(NH_3)_4Ru\}_2(bptz)]^{5+}$ complex being oxidized to the $[\{(NH_3)_4Ru\}(bptz)]^{+6}$ species. The chemical re-reduction ability of the [2, 3] or [3, 3] bimetallic complex to produce the absorption spectrum of the initial $[\{(NH_3)_4Ru\}_2(bptz)]^{4+}$ spectrum further substantiates the electrochemical reversibility of the ruthenium oxidations. Addition of excess Ce(IV) past the second equivalence point caused loss of the isosbestic point again, probably as a result of NH_3 oxidation to form NO, as has been reported for Ce(IV) oxidations of $(trpy)Ru(bpy)NH_3^{2+}$ [37]. Collaborative work is currently underway on electrochemical generation of mixed-valence intermediates of $[\{(NH_3)_4Ru\}_2(bptz)]^{5+}$ and previously prepared bimetallic complexes with large ΔE values.

The assignment of ^1H NMR signals for the bptz ligand is based on previous assignments for pyridine [38] and similar ligands such as dpp and dpq [15]. Tentative assignment of uncoordinated bptz signals has H_6 farthest downfield at 8.93 with coupling constants $J_{6,5} = 4.8$; $J_{6,4} = 1.9$ and $J_{6,3} = 1.1$ Hz. The H_3 resonance is at 8.68 ppm with $J_{3,4} = 7.8$; $J_{3,5} = 1.1$ Hz. H_4 is a set of overlapping doublets at 8.15 ppm and $J_{4,5} = J_{4,3} = 7.8$; $J_{4,6} = 1.9$ Hz and the H_5 multiplet is at 7.69 ppm with $J_{5,6} = 4.8$, $J_{5,4} = 7.8$ and $J_{5,3} = 1.1$ Hz. An instrumentally generated simulated spectrum using the coupling constants is presented for comparison with the observed ^1H NMR spectrum (Fig. 4). The ^{13}C NMR spectrum for uncoordinated bptz gives four signals for quaternary bptz (pyridine) carbon atoms that are tentatively assigned as C_6 at 151.3, C_4 at 138.0, C_3 at 126.9, C_5 at 124.8 ppm.

The ^1H NMR spectrum of the symmetric bimetallic complex has $H_{6'}$ at 9.06 ppm (doublet); $H_{3'}$ at 8.84 ppm (doublet); $H_{4'}$ at 8.07 ppm and $H_{5'}$ at 7.78 ppm (triplets). Signals for $H_{6'}$, $H_{3'}$, and $H_{4'}$, are downfield from the uncoordinated ligand, while the $H_{5'}$ signal moves slightly upfield upon complexation. The ^{13}C NMR spectrum for the bimetallic complex has downfield shifts from the free ligand for $C_{6'}$, $C_{3'}$, and $C_{5'}$ to 154.1, 128.6 and 126.1 ppm, respectively, while the signal for $C_{4'}$ moves upfield slightly to 137.0 ppm.

Assignments of ^1H and ^{13}C NMR signals for the unsymmetric monometallic compound are based on the resonances and coupling constants of the free ligand and for the bimetallic compound. Thus, ^1H doublets at 8.97 and 8.88 ppm are assigned to $H_{6'}$ and H_6, respectively, and $H_{3'}$ and H_3 doublets appear at 8.66 and 8.60 ppm, respectively. $H_{5'}$ and H_5 triplets are at 7.84 and 7.68 ppm. Triplets at 8.15 and 8.11 ppm are assigned as H_4 and $H_{4'}$ respectively, as $H_{4'}$ is expected to shift upfield upon coordination (as in the bimetallic complex). The ^{13}C NMR spectrum of the monometallic complex gives eight distinct signals, that are again assigned by analogy to the signals for the free ligand and the shifts noted for the bimetallic complex. Based on this analogy, the assignment of carbon resonances is $C_{6'}$ and C_6 at 154.0 and 150.9 ppm, respectively; $C_{4'}$ and C_4 at 138.4 and 137.9 ppm, respectively; $C_{3'}$ and C_3 at 128.6 and 127.2 ppm; $C_{5'}$ and C_5 at 125.3 and 124.6 ppm.

Acknowledgements

The authors wish to acknowledge the generous financial support of this work through a Bristol-Myers Company Grant of Research Corporation. R.R.R. thanks Professor Harold Jones, Department of Chemistry, Colorado College, Colorado Springs, CO for collection of NMR data.

References

1 Q. Jaradadt, K. Barqawi and T. S. Akasheh, *Inorg. Chim. Acta., 116* (1986) 63.

2 S. Kohlmann, S. Ernst and W. Kaim, *Angew. Chem., Int. Ed. Engl., 24* (1985) No. 8684.
3 W. Kaim and S. Kohlmann, *Inorg. Chem., 25* (1986) 3304.
4 S. Ernst, V. Kasack and W. Kaim, *Inorg. Chem., 27* (1988) 1146.
5 S. Ernst and W. Kaim, *Inorg. Chem., 28* (1989) 1520.
6 W. Kaim and S. Kohlmann, *Inorg. Chem., 29* (1990) 2909.
7 C. H. Braunstein, A. D. Baker, T. C. Strekas and H. D. Gafney, *Inorg. Chem., 23* (1984) 857.
8 K. J. Brewer, W. R. Murphy, Jr., S. R. Spurlin and J. D. Petersen, *Inorg. Chem., 25* (1986) 882.
9 R. R. Ruminski, T. Cockroft and M. Shoup, *Inorg. Chem., 27* (1988) 4026.
10 K. J. Brewer, W. R. Murphy, Jr. and J. D. Petersen, *Inorg. Chem., 26* (1987) 3376.
11 R. R. Ruminski and J. O. Johnson, *Inorg. Chem., 26* (1987) 210.
12 M. Shoup, B. Hall and R. R. Ruminski, *Inorg. Chem., 27* (1988) 200.
13 I. Wallace and R. R. Ruminski, *Polyhedron, 6* (1987) 1673.
14 R. R. Ruminski and R. T. Cambron, *Inorg. Chem., 29* (1990) 1575.
15 J. A. Baiano, D. L. Carlson, G. M. Wolosh, D. E. DeJesus, C. F. Knowles, E. G. Szabo and W. R. Murphy, Jr., *Inorg. Chem., 29* (1990) 2327.
16 D. P. Rillema, D. G. Taghdiri, D. S. Jones, C. D. Keller, L. A. Worl, T. J. Meyer and H. A. Levy, *Inorg. Chem., 26* (1987) 578.
17 R. Sahai, L. Morgan and D. P. Rillema, *Inorg. Chem., 27* (1988) 3495.
18 R. R. Ruminski and J. D. Petersen, *Inorg. Chem., 21* (1982) 3706.
19 E. V. Dose and L. J. Wilson, *Inorg. Chem., 17* (1978) 2660.
20 M. Hunziker and A. Ludi, *J. Am. Chem. Soc., 99* (1977) 7370.
21 C. Overton and J. A. Connor, *Polyhedron, 1* (1982) 53.
22 J. D. Petersen, W. R. Murphy, Jr., R. Sahai, K. J. Brewer and R. R. Ruminski, *Coord. Chem. Rev., 64* (1985) 261.
23 R. R. Ruminski, K. D. Van Tassel and J. D. Petersen, *Inorg. Chem., 23* (1984) 4380.
24 R. Nasielski-Hinkens, M. Benedek-Vamos, D. Maetens and J. Nasielski, *J. Organomet. Chem., 217* (1981) 179.
25 A. Masschelein, A. Kirsch-De Mesmaeker, C. Verhoeven and R. Nasielski-Hinkens, *Inorg. Chim. Acta, 129* (1987) L13.
26 A. J. Bard and L. R. Faulkner, *Electrochemical Methods,* Wiley, New York, 1980, Appendix C.
27 W. Butte and F. H. Case, *J. Org. Chem., 26* (1961) 4690.
28 D. M. Stanbury, O. Haas and H. Taube, *Inorg. Chem., 19* (1980) 518.
29 R. Ruminski, J. L. Kiplinger, T. Cockroft and C. Chase, *Inorg. Chem., 28* (1989) 370.
30 R. P. Thummel and S. Chirayil, *Inorg. Chim. Acta, 154* (1988) 77.
31 J. B. Cooper, D. B. MacQueen, J. D. Petersen and D. W. Wertz, *Inorg. Chem., 29* (1990) 3701.
32 C. Creutz and H. Taube, *J. Am. Chem. Soc., 91* (1969) 3988.
33 C. Creutz and H. Taube, *J. Am. Chem. Soc., 95* (1973) 1086.
34 J. E. Sutton and H. Taube, *Inorg. Chem., 20* (1981) 3125.
35 N. S. Hush, *Prog. Inorg. Chem., 8* (1967) 381.
36 D. E. Richardson and H. Taube, *Inorg. Chem., 20* (1981) 1278.
37 W. R. Murphy, Jr., K. Takeuchi, M. H. Barley and T. J. Meyer, *Inorg. Chem., 25* (1986) 1041.
38 J. W. Emsley, J. Feeney and L. H. Sutcliff, *High Resolution Nuclear Magnetic Resonance,* Vol. 2, Pergamon, New York, 1966, pp. 794, 994.